AD-A162 407 LAGRANGIAN BOUNDARY EQUATION AND UNSTEADY SEPARATION OF 1/1
ELLIPTICAL CYLINDER AT ANGLE OF ATTACK(U) FOREIGN
TECHNOLOGY DIV WRIGHT-PATTERSON AFB OH Y CHEN
UNCLASSIFIED 15 NOV 85 FTD-ID(RS)T-0634-85 F/G 20/4 NL

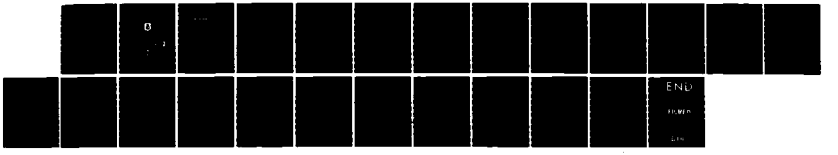

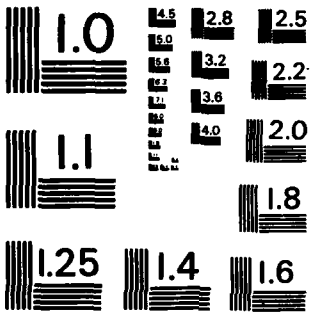

MICROCOPY RESOLUTION TEST CHART
NATIONAL BUREAU OF STANDARDS-1963-A

FTD-ID(RS)T-0634-85

FOREIGN TECHNOLOGY DIVISION

AD-A162 407

LAGRANGIAN BOUNDARY EQUATION AND UNSTEADY SEPARATION OF ELLIPTICAL CYLINDER AT ANGLE OF ATTACK

by

Chen Yunming

DTIC ELECTE DEC 18 1985 S D

DTIC FILE COPY

Approved for public release; distribution unlimited.

85 12 17 047

EDITED TRANSLATION

FTD-ID(RS)T-0634-85 15 Nov 85

MICROFICHE NR: FTD-85-C-001089

LAGRANGIAN BOUNDARY EQUATION AND UNSTEADY SEPARATION OF ELLIPTICAL CYLINDER AT ANGLE OF ATTACK

By: Chen Yunming

English pages: 20

Source: Shuxue Xuebao, Vol. 6, Nr. 11, 1983, pp. 571-578

Country of origin: China
Translated by: SCITRAN
F33657-84-D-0165
Requester: FTD/TQTA
Approved for public release; distribution unlimited.

THIS TRANSLATION IS A RENDITION OF THE ORIGINAL FOREIGN TEXT WITHOUT ANY ANALYTICAL OR EDITORIAL COMMENT. STATEMENTS OR THEORIES ADVOCATED OR IMPLIED ARE THOSE OF THE SOURCE AND DO NOT NECESSARILY REFLECT THE POSITION OR OPINION OF THE FOREIGN TECHNOLOGY DIVISION.

PREPARED BY:

TRANSLATION DIVISION
FOREIGN TECHNOLOGY DIVISION
WP-AFB, OHIO.

GRAPHICS DISCLAIMER

All figures, graphics, tables, equations, etc. merged into this translation were extracted from the best quality copy available.

Accesion For
NTIS CRA&I ☑
DTIC TAB ☐
Unannounced ☐
Justification .....
By .....
Dist.ibution /
Availability Codes
Dist | Avail and / or Special
A-1

QUALITY INSPECTED 3

/571

Lagrangian Boundary Equation and Unsteady Separation of Elliptical Cylinder at Angle of Attack

Chen Yunming

(Institute of Mechanics, Academia Sinica)

Abstract

In this ~~work~~, the Lagrangian boundary equation is introduced to steady the separation of an abruptly moved elliptical cylinder at the angle of attack. Not only the occurrence of separation singular points but also their forward movement with time were calculated. The computation also revealed that the separation pattern would change from trailing edge separation to leading edge separation. In regard to the methodology of computation, a transformation was introduced to map the non-uniform mesh on the physical plane to the uniform mesh on an auxiliary plane. Thus, it is only required to tighten the mesh (locally on the physical plane to improve the accuracy without increasing too much computing time. In addition, the advantages of the equal space finite difference, such as simplicity and high accuracy, will remain. Furthermore, a complicated variable boundary problem (separation point moving forward) was treated as a fixed boundary problem which significantly simplifies the process.

I. Boundary Layer Equation in Lagrangian Coordinates

In fluid dynamics, the Euler descriptive method is most commonly used because the majority of meaningful flow is steady.

Furthermore, the stress tension of a Newtonian fluid in Euler coordinates is simple. However, the Lagrangian method is also very useful for problems concerning separation with unsteady boundary layer, non-Newtonian fluids whose viscous tension is related to the microscopic history, or when specific particles in the fluid need to be tracked individually (such as turbulent diffusion).

In order not to complicate the problem, the discussion is limited to the unsteady two-dimensional boundary layer of an incompressible fluid. The following basic relations can be obtained from $x_\xi \xi_x + x_\eta \eta_x = 1$, $y_\xi \xi_x + y_\eta \eta_x = 0$:

$$\begin{aligned} \xi_x &= y_\eta / J \quad & \xi_y &= -x_\eta / J \\ \eta_x &= -y_\xi / J \quad & \eta_y &= x_\xi / J \end{aligned} \tag{1}$$

where $J = x_\xi y_\eta - x_\eta y_\xi$. In this case, the continuity equation is

$$u_\xi \xi_x + u_\eta \eta_x + v_\xi \xi_y + v_\eta \eta_y = 0 \tag{A}$$

From equation (1) and $u = x_t$ $v = y_t$, we get

$$\frac{\partial}{\partial t}(x_\xi y_\eta - x_\eta y_\xi) - \frac{\partial J}{\partial t} = 0 \tag{B}$$

Thus, the continuity equation becomes

$$J = x_\xi y_\eta - x_\eta y_\xi = 1 \tag{2}$$

Because the Jacobi determinant represents the area ratio of mapping, the above formula is the Lagrangian expression of the conservation of fluid volume.

Note that $\left(\frac{\partial}{\partial}\right)_x = x_\xi \frac{\partial}{\partial_\eta} - x_\eta \frac{\partial}{\partial \xi} = \frac{D}{D_y}$ then the boundary layer equation becomes

Manuscript received on April 5, 1983

1) This paper is dedicated to the 15th anniversary of the death of Professor Guo Yonghui.

/572

$$\left.\begin{aligned}\frac{\partial x}{\partial t} &= u \\ \frac{\partial u}{\partial t} &= -\frac{1}{\rho}p_x + \nu\left(\frac{D}{Dy}\right)^2 u\end{aligned}\right\} \tag{3}$$

We get the following by expanding the parenthesis

$$\begin{aligned}u_t = &-\frac{1}{\rho}p_x + \nu[x_\eta^2 u_{\eta\eta} - 2x_\xi x_\eta u_{\xi\eta} + x_\eta^2 u_{\xi\xi} - x_\xi u_\xi x_{\eta\eta} \\ &+ (x_\xi u_\eta + x_\eta u_\xi)x_{\xi\eta} - x_\eta u_\eta x_{\xi\xi}]\end{aligned} \tag{3'}$$

Note that equation (3) is not coupled to equation (2). It can be used independently to solve $x(\xi,\eta,t)$. In this case equation (2) can be used to find $y(\xi,\eta,t)$. The characteristic functions for equation (2) are

$$\frac{d\xi}{d\lambda} = -x_\eta, \quad \frac{d\eta}{d\lambda} = x_\xi, \quad \frac{dy}{d\lambda} = 1, \tag{A}$$

Hence, we know that $dx/d\lambda=0$. Thus, we can integrate along the x=constant curve to get

$$y = \int_{\text{壁面}}^{(\xi,\eta)} \frac{d\xi}{-x_\eta} = \int_{\text{壁面}}^{(\xi,\eta)} \frac{d\eta}{x_\xi} = \int_{\text{壁面}}^{(\xi,\eta)} \frac{ds}{\sqrt{x_\xi^2 + x_\eta^2}} \tag{4}$$

Let us assume that $x=\eta^2\varphi(\zeta)$ and $\zeta=(\xi+U_0 t)/\eta^2$; it is then possible to obtain the similarity solution to equation (3')-the steady motion of a semi-infinite plate (Blasius solution). From equations (2) and (3) it is also possible to get the Falker-Skan solution and the merging point flow. Nevertheless, the most noticeable advantage of the Lagrangian coordinate is in the treatment of unsteady boundary layer separation. With the exception of the classical case of two-dimensional steady

boundary, the criteria for boundary layer separation are still not yet clear. For instance, there are many types of separation of a three-dimensional steady boundary layer[1]. There were controversies on the separation of an unsteady two-dimensional boundary layer. In the late fifties, based on special cases (separation of steady boundary layer in solid wall motion), Sears et al introduced the M-R-S condition: $u=0$ and $\partial u/\partial y=0$ at separated points[2]. In the seventies, Sears and Tellionis used the divergence of numerical methods to determine the occurrence of singular points-the physical appearance of separation[3,4]. For instance, at a certain time after the cylinder begins to move ($t=2u\ t/R=1.3$) the calculation of a certain time in the flow field is divergent, a singular point appears. However, the computation performed by Cebeci et al could last until $t=2.8$[5]. They believed that the divergence of the computation performed by Tellionis et al is a problem of the specific scheme and does not necessarily have any physical significance. The problem became clearer after Shen Shenfu et al introduced Lagrangian coordinates to treat the problem[6].

In Lagrangian coordinates, a steady flow is also unsteady. Thus, it is possible to use one description for both steady and unsteady boundary layer separations. From equation (4) one can see that when a certain point in the flow field has the following properties

$$x_\xi = 0,\ x_\eta = 0 \qquad (5)$$

then the integral along the $x=x_s$ curve through this point is going to approach infinity (on the $1/\sqrt{Re}$ scale). The above formula shows that the fluid masses near (ξ_s,η_s) reach the same

position $x=x_s$ in the x-direction at the same time. Because the volume is invariant, thus it extends to infinity in the y-direction. It seems to have an unsurmountable obstacle in the x-direction. The fluid masses cannot continue forward. They are separated from the body and move toward infinity in the y-direction (on the scale of $1/\sqrt{Re}$). This is the definition of separation given by Prandtl earlier.

In the following we will prove that equation (5) is valid for separation of a steady flow in a solid wall movement. It is obvious we have

$$t = \int_{\xi}^{x} \frac{dx}{u(x, \psi)} = t(x, \psi, \xi) \tag{6}$$

$$\left.\begin{aligned} t_x x_\xi + t_\psi \psi_\xi + t_\xi = 0 \\ t_x x_\eta + t_\psi \psi_\eta = 0 \end{aligned}\right\} \tag{7}$$

/573

If $u(x_s, \varphi_s)=0$ in the flow field (not in the solid wall $x \neq \xi$), from equation (6) we know that $t_x \to \infty$. Based on equation (7), equation (5) must be satisfied. We also have $u_y = x_\xi u_\eta - x_\eta u_\xi = 0$, i.e., the M-R-S condition.

In Lagrangian coordinates, the separation condition (5) shows that a separation point is an extremum of $x(\xi, \eta)$, instead of a singular point (a singular point appears only when we try to determine y and y is not needed in calculating x). Therefore, there is no difficulty and ambiguity in the numerical computation. It is clearly indicated in reference [6] that cylinder separation begins to emerge at $\bar{t}=3.0$ and $\theta_s \simeq 111°$.

II. Unsteady Separation of Elliptical Cylinder with Angle of Attack

In the following we will extend the above one step further to apply the Lagrangian coordinate to calculate the unsteady separation of an abruptly moved elliptical cylinder with angle of attack. There are two objectives: first we not only want to calculate the occurrence of an unsteady separation but also to track it with time. Next, we want to study the variation of the position of separation with angle of attack. That means when the angle of attack is increased, it changes from trailing edge separation to leading edge separation (which is the cause of stalling of aircrafts). As the first step, we temporarily neglected to reverse influence of separation on the pressure distribution, which is allowed in the initial stage of separation. This reverse influence is taken into account in the next step. Because the calculation of pressure distribution is an independent subroutine, taking the reverse influence into account has no effect on the numerical solution of the boundary layer itself. It is essentially a problem to accurately simulate the separation vortex in the external flow, which is another special topic to be specially discussed elsewhere.

In the following, physical quantities with ' represent dimensional parameters and those without ' are dimensionless quantities. First, we introduced an elliptical coordinate to use φ to replace the arc length x' to describe the points on the surface of the ellipse, i.e., to change variables from (ξ,η) to (φ_0,η). The unknown function is still x (which is a function

of φ). In a Cartesan coordinate $(\tilde{x},\tilde{y})$, an ellipse is $\tilde{x}$=a cosφ and $\tilde{y}$=b sinφ (where a and b are the long and short axes). The arc length of the ellipse is

$$x' = \int_0^{\psi} \sqrt{a^2 \sin^2\psi + b^2 \cos^2\psi}\, d\psi, \qquad \text{(A)}$$

It is rendered non-dimensional as

$$x(\psi) = \frac{2x'}{a+b} = \int_0^{\psi} \sqrt{E_0 + E_2 \sin^2\psi}\, d\psi \qquad (8)$$

where $E_0 = (2b/a+b)^2$, and $E_2 = 4$ a-b/a+b. The inverse is noted as φ (x). In this case the variables are $\xi = x(\varphi_0)$ and $\varphi_0 = \varphi(\xi)$. The non-dimensional potential velocity is

$$U(\psi) = \frac{u'}{2u_\infty} = \frac{\cos\alpha \sin\psi + \sin\alpha \cos\psi}{\sqrt{E_0 + E_2 \sin^2\psi}} \qquad (9)$$

where α is the angle of attack. The origin is placed at the apex of the α semi-axes. Therefore, the leading edge stagnation point is $\varphi = -\hat{\alpha}$, $x_0 = x(-\hat{\alpha}) = -x(\hat{\alpha})$. The time is rendered dimensionless as $t = 4u_\infty t/a+b$. The ordinate is also made non-dimensional as $y = 2y'/a+b \sqrt{u_\infty (a+b) / \nu}$. The non-dimensional velocity is $u = u'/2u_\infty$.

Next, the following transformation is introduced to map the semi-infinite plane $(-\hat{\alpha} \leq \varphi_0 < \pi - \hat{\alpha}, 0 \leq \eta < +\infty)$ to the square $(0 \leq \alpha \leq 1,\ 0 \leq \beta \leq 1)$:

$$\left.\begin{aligned}\psi_0 &= C\left[h_1 \operatorname{arctg}\left(h_2 \operatorname{tg}\frac{\pi\alpha}{2}\right)-\alpha\right]-\hat{\alpha}\\ \eta/\delta &= \operatorname{tg}\frac{\pi\beta}{2},\quad \delta = 2\sqrt{\nu t/(1+\lambda t)}\end{aligned}\right\} \tag{10}$$

where C, h_1 and h_2 are constants. $h_1 = 4(1+d)/(\pi h_2(2+d))$, and $h_2 = \sqrt{d/(2+d)}$ which make /574

$$\frac{d\alpha}{d\psi_0} = (1+d+\cos\pi\alpha)/C(1+d-\cos\pi\alpha)) \tag{A}$$

simple. C should be chosen so that $\psi_0 = \pi - \hat{\alpha}$ when $\alpha=1$(in our calculation d=0.55 and C=1.942).

Boundary Conditions: conditions for the leading edge and trailing edge stagnation points and the wall surface are

$$\left.\begin{aligned}&\alpha = 0,\ 1(\psi = -\hat{\alpha},\ x = \hat{\alpha}): u = 0,\ x = \xi\\ &\beta = 0: u = 0,\ x = \xi\end{aligned}\right\} \tag{11}$$

At infinity, $\beta=1$, $u=U(\varphi)$ and $x=x(\xi,\eta=\infty,\ t)$. Fortunately, an integral expression can be found for $x(\xi,\eta=\infty,t)$ to simplify the computation program. From

$$t = \int \frac{dx}{U} = \int \frac{d\psi}{\sin(\psi+\hat{\alpha})}(E_0 + E_2\sin^2\psi) = \int E_3 d\ln\operatorname{tg}\frac{\psi+\hat{\alpha}}{2} - E_2\cos(\psi-\hat{\alpha}) \tag{B}$$

we get

$$t = E_3 \ln\frac{\operatorname{tg}[(\psi+\hat{\alpha})/2]}{\operatorname{tg}[(\psi_0+\hat{\alpha})/2]} - E_2[\cos(\psi-\hat{\alpha}) - \cos(\psi_0-\hat{\alpha})] \tag{12}$$

where $E_3 = E_0 + E_2\sin^2\hat{\alpha}$. $\varphi_0 = \varphi(\xi)$ is already known. When t is given, and $x(\varphi)$ can be determined.

Velocity distribution and displacement thickness: when x remains unchanged, the following can be calculated for each increment

$$\Delta\xi = \frac{\partial\xi}{\partial y}\Delta y = -x_\eta\Delta y,\quad \Delta\eta = x_\xi\Delta y. \tag{C}$$

Starting from the wall, $\xi_0 = x$, $\eta_0 = 0$, $\xi_1 = \xi_0 - x_\eta \Delta y$, $\eta_1 = \eta_0 +$ (D) $x_\xi \Delta y, \ldots \ldots, \xi_\eta = \xi_{n-1} - (x\eta)_{n-1}\Delta y$, $\eta_n = \eta_{n-1} + (x_\xi)_{n-1}\Delta y$, $u(\xi_n, \eta_n)$ $u(x, n\Delta y), \ldots\ldots$ With $u(x,y)$, it is not difficult to calculate the displacement thickness δ_1.

III. Numerical Method

Under the transformation (10), the basic equation (3') becomes

$$u_t = U(\psi)U'(\psi)/x'(\psi) + \alpha_\xi^2\beta_\eta^2[x_\alpha^2 u_{\beta\beta} - 2x_\alpha x_\beta u_{\alpha\beta} + x_\beta^2 u_{\alpha\alpha} - x_{\alpha\alpha}u_\alpha x_{\beta\beta} + (x_\alpha u_\beta + x_\beta u_\alpha)x_{\alpha\beta} - x_\beta u_\beta x_{\alpha\alpha} + (x_\alpha u_\beta - x_\beta u_\alpha) \cdot (x_\alpha\beta_{\eta\eta}/\beta_\eta^2 - x_\beta\alpha_{\xi\xi}/\alpha_\xi^2)] - \beta_t u_\beta \quad (13)$$

Because there is a circular flow area on the flow field, therefore, it is necessary to have corresponding countermeasures in the difference scheme and integration method.

1. Difference Scheme: An implicit difference scheme (Crank-Nicholson) is used for partial derivatives of time. A center difference scheme is used for $x_{\alpha\alpha}$, $x_{\beta\beta}$, $x_{\alpha\beta}$, x_α, x_β, $u_{\alpha\alpha}$, $u_{\beta\beta}$, and $u_{\alpha\beta}$. However, a tail wind difference scheme is used for u_α and u_β terms, i.e., forward difference if the coefficient is positive and backward difference if otherwise. Thus, the difference equation can be stabilized.

2. Because the equation is non-linear, its coefficients are related to unknown functions. They must be solved by iteration. We used the Gauss-Sider iteration method to solve the difference equation. In each iteration, n simultaneous algebraic equations are solved for a specific α value (i.e., a specific x position).

n is the number of mesh points in the β-direction. After u and x are determined, the equation for the next α is integrated to complete the iteration step by step from one end to the other. However, the direction of integration of α is changed after each iteration: if it is from α=1 to α=0, then the next time integrate from α=0 to α=1. Because the effect of the circular flow comes from both sides, this method can quickly spread the effect of boundary conditions to every point. Our experience shows that this can significantly accelerate the rate of convergence.

3. Because the motion is started abruptly, it is a singular point at t=0. The proper selection of an initial value when t is very small can ensure the accuracy of the entire computation. The details are discussed in reference [6].

4. Determination of Point of Separation /575

The conditions for the first occurrences of separation (singular point) are

$$\Omega = \partial u/\partial y = 0 \text{ and } D = x_{\xi\xi}x_{\eta\eta} + x_{\xi\eta}^2 = 0 \qquad (A)$$

The deviation is in reference [6]. However, D=0 is no longer true at the point of separation at later times. Therefore, we used the direct condition (5) to determine the point of separation. With known x_ξ and x_η values on a mesh point, the intersect of x_ξ=0 and x_η=0 can be determined by intrapolation. There are usually two intersects, corresponding to the positive and negative values of D. The intersect corresponding to D<0 is the true point of separation. As shown in Figure 5, there is

another point where $x_\xi=0$ and $x_\eta = 0$, on the inside of the enclosed curve (which corresponds to points outside the boundary layer as discussed in 3). This point is the minimum of $x(\xi,\eta,t)$. Thus, D> 0.

5. Choice of Mesh Number: N_ξx N_η x Δt.

Doubling N_ξ or N_η will nearly double the computation time. N_ξ primarily affects the resolution in the ξ direction, which is mainly determined by the extent of pressure variation. N_η is primarily determined by velocity distribution and by τ_ω. For instance, the circular flow region extends in the η direction at large attack angles. Therefore, N_ξ should be increased. The final N_ξ, N_η and Δt are determined by trial runs (i.e., doubling the meshes without affecting the result significantly).

IV. Results and Discussion

1. Trailing Edge Separation - Leading Edge Separation.

Computations are made at three angles of attack (with the semi-axis ratio of the ellipse b/a = 0.5).

At zero angle of attack, $\hat{a}=0$, separation occurs at the trailing edge at $x = 2x'_s/(a+b) = 2.85$ (the semi-circumference is 3.23). Several transformations $\alpha(\xi,t)$ and $\beta(\xi,\eta,t)$ were attempted and results showed that the one recommended in the second section is better. It does not add too much computing time but can maintain better accuracy. The movement of the point of separation with time, $x_s \sim t_s$, as well as a comparison of δ_1 and τ_ω at separation and their corresponding known solutions are

shown in Figure 1. Results obtained using two different meshes, 65x17x0.05 and 73x33x0.0125, are in good agreement. The time at which separation occurs is $t_s \simeq 1.8$.

At a medium angle of attack of $\hat{\alpha}=22.92°$, separation still occurs in the trailing edge, as shown in Figure 2. Another transformation was attempted when the angle of attack exists to make the mesh points closer near the apex of the semi-axis.

$$\psi = C\left[h_1 \operatorname{arctg}\left(h_2 \operatorname{tg}\frac{\pi(\alpha-\alpha_0)}{2}\right) - (\alpha-\alpha_0)\right] \qquad (B)$$

where C and α_0 are determined by $\alpha=0$ at $\varphi=-\hat{\alpha}$ and $\alpha=1$ at $\varphi=\pi-\hat{\alpha}$. However, the result is not as good as that obtained using equation (10). At a medium angle of attack, the pressure gradient near the leading edge is not sufficient to cause separation. But, the trailing edge is not sufficient to cause separation. But, the trailing edge stagnation point is shifted to the flat position of the ellipse where separation shows up very late at $t_s \simeq 3.8$ because the pressure variation is slow. The mesh remains to be 65x17x0.05. After tightening the mesh in the β -direction by one fold, x_s, t_s and u_s do not change by one percent. As the trailing edge singularity is developing (i.e., grad x is decreasing but not yet zero), the singularity near the leading edge (where pressure varies violently) is also developing, but much slower.

The separation at a large angle of attack of $\hat{\alpha}=50°$, just as expected, occurs at the leading edge where pressure fluctuates violently. The ratio of the distance from the leading edge

stagnation point to the separation point, $x(\hat{a})+x_s$, to the semi-circumference is 0.32. Consequently, the time of separation also arrives much earlier; $t_s \simeq 2.1$. In this case, the backflow area and separation point are far away from the wall. Therefore, the mesh is increased to 65x65x0.05 (not too different from the result obtained with the 65x33x0.05 mesh). The calculated results are shown in Figure 3. As the leading edge singularity (i.e., decreasing grad x) is developing, there is trailing edge singularity underdevelopment.

Summarizing the three cases above, separation always occurs in the rear half when $\hat{a}$ is not large. While after $\hat{a}$ exceeds a certain critical value a_c, separation will occur in the front half. In this case, t_s will also decrease. Therefore, the variation of t_s with the angle of attack is as the $t_s \sim \hat{a}$ curve shown in Figure 4. The jump of the value of t_s at $a=\hat{a}_c$ is caused by the "jump" of the point of separation from the rear of the cylinder to the front. Similar "jump" phenomena also occur with the steady separation of an ellipse[1]. From this study we know that singularities can develop in front and rear of the body due to an inverse pressure gradient (decreasing grad x with increasing y-axis). Where separation occurs depends on where the /576 singularity develops faster. Singularity does not occur in one place and this singularity will "jump" from the rear to the front.

2. How to Improve Accuracy

The special feature of the Lagrangian coordinate is that the

mesh on the (ξ,η) plane varies with time. The mesh near the leading edge stagnation point becomes larger as the masses move downstream. Therefore, the mesh should be closer. Next, in order to improve resolution, the mesh should also be closer near the apex of the α semi-axis where the pressure varies violently. However, too many mesh points will lead to excessive computing time. If the mesh is only tightened locally, not only the difference scheme is complicated but also the accuracy is affected due to the fact that the mesh is non-uniform (for instance the center difference is no longer accurate to the second order). We solved the problem by introducing the transformation (10) and an elliptical coordinate (8) to make a uniform mesh on the (α,β) plane to become the non-uniform mesh on the (ξ,η) plane - tightened at the semi-axis apex and the leading edge stagnation point. In this case, although the equations are complicated, yet logarithmic calculations will not bring about any difficulty in substance.

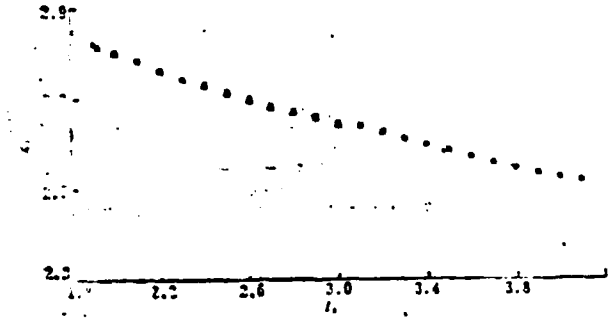

Figure 1a $\hat{\alpha}$=0°
X73X33X0.0125 Δ65X17X0.05

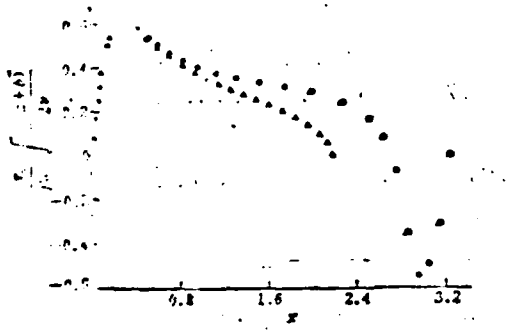

Figure 1b $\hat{\alpha}$=0°, t=1.75
o 73X33X0.0125 Δsteady solution

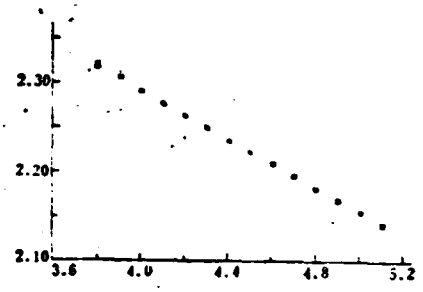

Figure 2 $\hat{\alpha}$=22.9°
o 65X17X0.05 Δ65X33X0.05

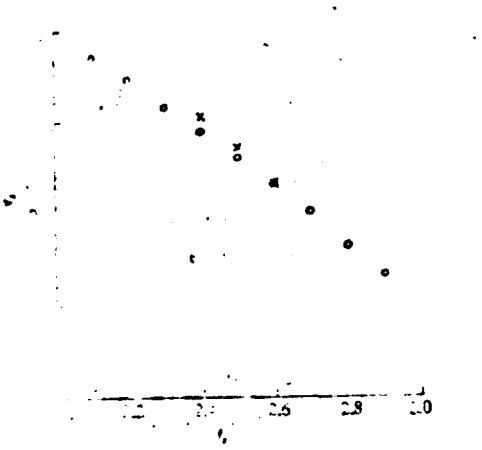

Figure 3a $\hat{\alpha}$=50°
o 65X65X0.05 X 33X33X0.1

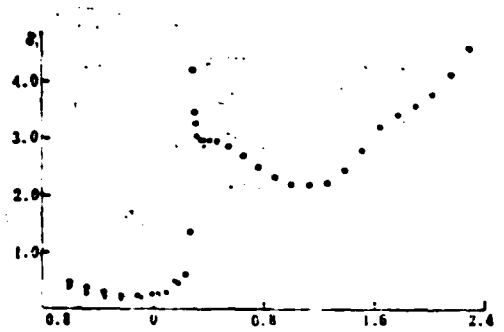

Figure 3b $\hat{\alpha}$=50°, 65X65X0.05
o t=2.1 X t=2.7

3. Variable Boundary Problem - Steady Boundary Problem /577

In the Euler method, this is a variable boundary problem on the (x,y) plane plane which should be integrated from x=0 to $x=x_s$ and x_s decreases with time. This problem is very complex. In the Lagrangian method, this is also a variable boundary problem on the (ξ,η) plane. However, it can be treated as a steady boundary problem, still integrating from α=0 to α=1. The contour of the solution $x(\xi,\eta,t)$ after separation is shown in Figure 5. The solution $x(\xi,\eta,t)$ itself is normal on the (ξ,η) plane. It corresponds to finding y by integrating (4) along the curve x=constant on the physical plane (x,y). However, it is not possible to enter the enclosed curve $x=x_s$ starting from the solid wall, i.e., points inside the curve are outside the boundary

layer (which is infinity on the scale of $\sqrt{Re}$). The x values on these points, in some sense, can be considered as the analytical extension of the x values of external points.

4. Intensity of Separated Vortex

At a specific time t , points inside the singular curve $x(\xi,\eta,t_0)=x$ correspond to separated points. However, at a separated singular point (ξ_s,η_s) $\partial u/\partial y=0$, $u_s\neq 0$ and $\eta_s\neq 0$ (not on the wall). In this case, below it we have ($x=x_s$, $\eta<\eta_s$) $\partial u/\partial y<0$. Furthermore, the y value calculated according to equation (4) is finite. Therefore, this part is not separated. Furthermore, only the part above it is separated ($x=x_s$, $\eta>\eta_s$ and $\partial u/\partial y>0$). According to the M-R-S condition, in the coordinate in motion at ($w'=u'-u_s'$), we have $w'=0$ and $\partial w'/\partial y=0$. In addition, the vortex flux separated from the boundary layer to enter the external flow is $\int_{y_s}^{\infty} w'\partial w'/\partial y\, dy = w'^2=\frac{1}{2}(u'-u')^2$. The intensity of the separated vortex can thus be determined. It provides an important parameter for the next step to take the inverse effect of separated vortex on the pressure distribution into consideration. After each step Δt, it is possible to calculate the newly increased separated vortex intensity. (How to simulate separated vortex and its movement is another topic.) Based on the separated vortex, we can calculate a new pressure distribution. The new pressure distribution can be used in the numerical integration in the next step Δt.

This work was performed under the guidance of Professor Shen Shenfu. The author wishes to thank Dr. Van Dommelen for his unselfish assistance during the course of this work.

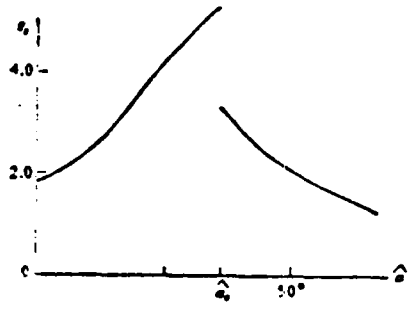

Figure 4

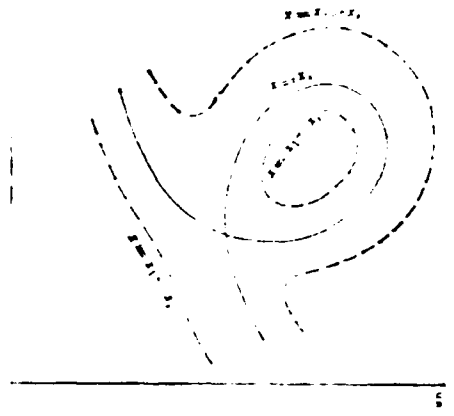

Figure 5. The Contour

References

[1] Wang, K.C., J. AIAA, 10(1972), 33.

[2] Moore, F.K., In Boundary Layer Research, Gortler, H. ed. (1958), 296.

[3] Seare, W. R. and Telionis, D. P., In Recent Research on Unsteady Boundary Layers, Eichelbrenner, E.A. ed. (1971), 404.

[4] Telionis, D. P. and Teahalis, D. Th., Acta Astronautica, 1(1974), 1487.

[5] Cebeci, T., J. Comp. Phys., 31(1979), 153.

[6] Van Dommelen, L. L. and Shen, S. F., J. Comp. Phys., 38(1980), 125.

THE LAGRANGIAN BOUNDARY LAYER EQUATION AND THE UNSTEADY SEPARATION OF THE ELLIPTIC CYLINDER AT ANGLE OF ATTACK

Chen Yunming

(Institute of Mechanics, Academia Sinica)

Abstract

Lagrangian coordinates were introduced to investigate the unsteady boundary layer separation of elliptic cylinder at angle of attack. The forward-movement of the separation point with time was calculated. As well as the first occurrence of separation. It was also found that the separation pattern would change, as expected, from rear-separation to fore-separation as the angle of attack increased.

In respect to the numerical methodogy, coordinate transformations were introduced to map the nonuniform mesh points in the physical plane to the uniform mesh points in the auxialliary plane to simplify the finite difference formula, and the complicated moving-boundary problem was treated in a fixed-boundary manner.

END

FILMED

2-86

DTIC